Journal of Molecular and Cellular Cardiology 76 (2014) 247–256

Contents lists available at ScienceDirect

Journal of Molecular and Cellular Cardiology

journal homepage: www.elsevier.com/locate/yjmcc

Original article

Intracellular Na^+ overload causes oxidation of CaMKII and leads to Ca^{2+} mishandling in isolated ventricular myocytes

Serge Viatchenko-Karpinski [a,*], Dmytro Kornyeyev [a], Nesrine El-Bizri [a], Grant Budas [a], Peidong Fan [a], Zhan Jiang [a], Jin Yang [b,c], Mark E. Anderson [d,1], John C. Shryock [a,2], Ching-Pin Chang [b,c], Luiz Belardinelli [a], Lina Yao [a,**]

[a] Department of Biology, Gilead Sciences, Fremont, CA 94555, USA
[b] Krannert Institute of Cardiology and Division of Cardiology, Indiana University School of Medicine, Indianapolis, IN 46202, USA
[c] Department of Medicine, Indiana University School of Medicine, Indianapolis, IN 46202, USA
[d] University of Iowa Carver College of Medicine, Department of Internal Medicine, Iowa City, IA 52242, USA

ARTICLE INFO

Article history:
Received 24 March 2014
Received in revised form 7 July 2014
Accepted 11 September 2014
Available online 22 September 2014

Keywords:
Late sodium current
ATX-II
RyRs
CaMKII
ROS
Mitochondria

ABSTRACT

An increase of late Na^+ current (I_{NaL}) in cardiac myocytes can raise the cytosolic Na^+ concentration and is associated with activation of Ca^{2+}/calmodulin-dependent protein kinase II (CaMKII) and alterations of mitochondrial metabolism and Ca^{2+} handling by sarcoplasmic reticulum (SR). We tested the hypothesis that augmentation of I_{NaL} can increase mitochondrial reactive oxygen species (ROS) production and oxidation of CaMKII, resulting in spontaneous SR Ca^{2+} release and increased diastolic Ca^{2+} in myocytes. Increases of I_{NaL} and/or of the cytosolic Na^+ concentration led to mitochondrial ROS production and oxidation of CaMKII to cause dysregulation of Ca^{2+} handling in rabbit cardiac myocytes.

1. Introduction

Regulation of cellular sodium (Na^+) and calcium (Ca^{2+}) handling is essential for the maintenance of normal excitation–contraction coupling [1–3]. Cardiac Na^+ channels open transiently and inactivate rapidly, causing a large, brief peak of Na^+ current that initiates the cardiac action potential [4,5]. Under pathological conditions, including heart failure and myocardial ischemia, Na^+ channel inactivation is slowed and/or incomplete, resulting in a sustained Na^+ current, referred to as persistent or late Na^+ current (I_{NaL}) [3–5]. Increased I_{NaL} promotes intracellular Na^+ overload, thereby reducing the electrochemical gradient for Ca^{2+} extrusion by the Na^+–Ca^{2+} exchanger (NCX), causing cellular Ca^{2+} overload, contractile dysfunction, and arrhythmias [3–5].

In addition to increasing cytosolic Ca^{2+}, intracellular Na^+ overload also perturbs mitochondrial Ca^{2+} homeostasis, resulting in mitochondrial reactive oxygen species (ROS) generation [6–8]. Ca^{2+} is an important regulator of the mitochondrial redox state [6–10]. Ca^{2+} activates key rate-limiting enzymes of the Krebs cycle (pyruvate, isocitrate, and malate dehydrogenases) required for producing NADH (the main electron donor for ATP in the respiratory chain) and for regenerating NADPH (to maintain the antioxidative capacity of mitochondrial matrix enzymes) [9]. When cardiac work increases, mitochondrial Ca^{2+} uptake is elevated to increase the Krebs cycle activity and ATP production to meet an increased metabolic demand [9]. An elevation of the cytosolic [Na^+], on the other hand, decreases mitochondrial Ca^{2+} uptake and NADH levels [6]. In myocytes isolated from failing hearts, cytosolic Na^+ elevation promotes mitochondrial Ca^{2+} efflux via the mitochondrial Na^+–Ca^{2+} exchanger, and thereby reduces the Krebs cycle activity and levels of NADH and NADPH [6,7]. A decrease in the level of NADPH impairs the capacity of antioxidant enzymes such as thioredoxin and glutathione to reverse protein oxidation, thus increasing ROS-induced cellular dysfunction. Indeed, the elevated ROS in cardiomyocytes isolated from the failing heart can be normalized either by lowering cytosolic [Na^+] or by inhibiting mitochondrial Na^+–Ca^{2+} exchange [7,8,10]. Conversely, elevating cytosolic Na^+ increases ROS generation in normal cardiomyocytes [7]. These studies suggest that mitochondrial ROS

* Correspondence to: S. Viatchenko-Karpinski, Department of Biology, Gilead Sciences, Inc., 7601 Dumbarton Circle, Fremont, CA 94065, USA. Tel.: +1 510 739 8453; fax: +1 510 739 8401.
** Correspondence to: L. Yao, Department of Biology, Gilead Sciences, Inc., 7601 Dumbarton Circle, Fremont, CA 94065, USA. Tel.: +1 510 739 8437; fax: +1 510 739 8401.
E-mail addresses: Serge.Karpinski@gilead.com (S. Viatchenko-Karpinski), Lina.Yao@gilead.com (L. Yao).
[1] Present address: John Hopkins University, Department of Medicine, MD, 21287, USA.
[2] Present address: 3420 SW 77th Street, Gainesville, FL 32608, USA.

http://dx.doi.org/10.1016/j.yjmcc.2014.09.009

generation may play a critical contributory role in mediating the pathological effects of cytosolic Na^+ overload [2,7,8,10].

Elevated ROS production promotes adverse cardiac remodeling by activating intracellular signaling pathways that induce cardiomyocyte cell death, hypertrophy, and arrhythmia [11]. We previously demonstrated that the multi-functional Ca^{2+}/calmodulin-dependent protein kinase II delta (CaMKIIδ) is activated in response to enhanced I_{NaL} and mediates downstream pathological processes that include necrotic and apoptotic cardiac cell death and ventricular arrhythmia [12]. CaMKIIδ phosphorylates a number of substrates involved in cellular Ca^{2+} homeostasis, including phospholamban (PLN), the sarcoplasmic reticulum (SR) Ca^{2+}ATPase, ryanodine receptor 2 (RyR2), and the cardiac Na^+ channel, $Na_v1.5$. Phosphorylation of these proteins disrupts normal SR Ca^{2+} cycling, promotes cellular Ca^{2+} overload, induces spontaneous Ca^{2+} release, and alters excitation–contraction coupling and propagation of electrical impulses [13–18]. CaMKIIδ activity is regulated by Ca^{2+}/calmodulin and depends on the amplitude and frequency of cytosolic Ca^{2+} waves. CaMKIIδ activity is also regulated by direct oxidation of methionine 281/282 at its regulatory domain [11,15]. Based on its dual modes of activation, CaMKIIδ is centrally poised to sense elevations in either Ca^{2+} or ROS, and to initiate downstream molecular events that promote Ca^{2+} mishandling. CaMKIIδ may therefore serve as a nodal point of convergence for pathological signaling events induced by an increased I_{NaL} [12,18].

Despite the well-established link between cytosolic Na^+ overload and altered intracellular Ca^{2+} handling [3–8,12,19–21], the mechanism of Na^+-dependent modulation of Ca^{2+} dynamics is not fully understood [2]. In this study we tested the hypothesis that intracellular Na^+ overload caused by an enhanced I_{NaL} increases mitochondrial ROS production, resulting in oxidation-induced activation of CaMKIIδ that in turn promotes Ca^{2+} mishandling. Our experimental approaches to study the pathway between intracellular Na^+ overload and Ca^{2+} mishandling included intact and permeabilized adult rabbit cardiomyocytes exposed to an enhancer of I_{NaL} and an increased superfusate Na^+ concentration, respectively, and a mouse model of pressure overload-induced heart failure. Fluorescent dyes sensitive to Na^+, Ca^{2+}, and ROS were used to measure the effects of increased I_{NaL} and intracellular Na^+ to alter ROS formation and cellular Ca^{2+} handling. *Anemonia sulcata* toxin II (ATX-II) and ranolazine were used to increase and inhibit I_{NaL}, respectively [22,4].

2. Materials and methods

2.1. Chemicals

ATX-II and tetrodotoxin were purchased from Alomone Labs and Tocris Bioscience, respectively. Dithiothreitol (DTT) and coenzyme Q10 (CoQ10) were purchased from Sigma Chemical. The CaMKII inhibitor KN-93 and its inactive analog KN-92 were purchased from EMD Millipore. Ranolazine and the selective I_{NaL} blocker GS-967 [23] were provided by Gilead Sciences. The sources of fluorescent dyes and antibodies are indicated in the relevant sections below.

2.2. Cell isolation

Experimental protocols using animals were approved by the Gilead Institutional Animal Care and Use Committee following the criteria outlined in the National Institutes of Health Guide for the Care and Use of Laboratory Animals (NIH Publication No. 85-23, revised 1996). Adult female 2–3 kg New Zealand White rabbits (Western Oregon Rabbit Company) were sedated with intramuscular injections of 35 mg/kg ketamine and 5 mg/kg xylazine. The respiratory rate, muscle tone, and righting reflex were monitored to ensure sedation. Once sedated, rabbits were given 1 mL of heparin (1000 USP units/mL) into the ear vein and then deeply anesthetized by intravenous injection of 15 mg/mL ketamine and 3 mg/mL xylazine. Hearts were removed and mounted on a Langendorff apparatus for retrograde perfusion (17–20 mL/min) of the aorta with a perfusion solution containing (in mmol/L): 140 NaCl, 4.4 KCl, 1.5 $MgCl_2$, 1 NaH_2PO_4, 5 HEPES, 7.5 glucose, 16 taurine, 5 Na pyruvate, and NaOH to adjust the pH to 7.3. Cardiac myocytes were enzymatically isolated from left ventricles as previously described by Brunner et al. [24]. The perfusion solution was supplemented with collagenase type II enzyme (0.8 mg/mL, Worthington), 0.2% 2,3-butanedione monoxime, and 0.2% bovine serum albumin. Left ventricles were dissected, chopped, and subjected to postdigestion in a shaker with periodical changes of an isolation solution. The isolation solution contained (in mmol/L): 140 NaCl, 4.6 KCl, 1.1 $MgCl_2$, 1 NaH_2PO_4, 10 HEPES, 10 glucose, and NaOH to adjust the pH to 7.4. The isolation solution was supplemented with a low concentration (0.344 mg/mL) of collagenase and 0.975% albumin. All procedures were performed at 37 °C. Isolated cardiomyocytes were used within 6 h after isolation.

Adult male mice were heparinized and sacrificed by cervical dislocation. The hearts were perfused on the Langendorff apparatus with the following solution (in mmol/L): 135 NaCl, 4.6 KCl, 1.1 $MgCl_2$, 1 NaH_2PO_4, 10 HEPES, 10 glucose, and NaOH to adjust the pH to 7.4. Then hearts were perfused with a solution supplemented with 0.896 mg/mL collagenase, 0.08 mg/mL protease type XIV, and 0.68 mg/mL bovine serum albumin for 15–20 min at 29 °C. The left ventricles were dissected and gently triturated. Isolated cardiomyocytes were used within 4 h after isolation.

2.3. Patch-clamp experiments

The whole-cell configuration of the patch-clamp technique was used to record I_{Na} in the voltage-clamp mode using a Multiclamp 700B amplifier (Molecular Devices) and pClamp 10.2 data acquisition software (Molecular Devices). The digital data were analyzed using pClampfit 10, Microcal Origin (OriginLab), and GraphPad Prism (Graph Pad Software) programs. Patch pipettes were pulled from a borosilicate glass (World Precision Instruments) using a DMZ Universal puller (Dagan). For the recording of I_{Na}, cardiomyocytes were superfused with a bath solution containing (in mM): 135 NaCl, 4.6 CsCl, 1.8 $CaCl_2$, 1.1 $MgSO_4$, 10 HEPES, 10 glucose, and 0.01 nitrendipine (pH 7.4 adjusted with NaOH). Pipette resistance was 1.5–2 MΩ when filled with a pipette (internal) solution containing (in mM): 120 aspartic acid, 20 CsCl, 1 $MgSO_4$, 4 $ATPNa_2$, 0.1 $GTPNa_3$, and 10 HEPES (pH 7.3 adjusted with CsOH). The recordings of I_{Na} were performed at 22–24 °C following a stabilization period (5–10 min) after establishing a patch with whole-cell configuration. The myocytes were held at −120 mV and depolarizing pulses (−20 mV, 220 ms) were applied at a rate of 1 Hz. The rate of decay (inactivation) of I_{Na} was fitted using two exponential terms, and the slower component was used to describe I_{NaL}.

2.4. Measurement of intracellular dye fluorescence

Experiments were performed using a LSM 5 PASCAL (Carl Zeiss) laser scanning confocal system equipped with a Zeiss Plan-Apochromat 40× 1.4 numerical aperture oil immersion objective. Myocytes were maintained in a bath solution containing (in mmol/L): 140 NaCl, 5.4 KCl, 2.0 $CaCl_2$, 2.5 $MgCl_2$, 10 HEPES and 5.6 glucose, pH 7.3. Cells were incubated for 25 min at 23 °C in the bath solution supplemented with 0.25 mmol/L $CaCl_2$, 2.5 μmol/L pluronic acid (Life Technologies) and the appropriate fluorescent dye, either 5 μmol/L Fluo-4 AM (Life Technologies), 5 μmol/L Asante NaTRIUM Green AM, Asante NaTRIUM Green-2 AM (Teflabs), 10 μmol/L 2′,7′-dichlorofluorescein diacetate (DCFDA; Life Technologies), or 2 μmol/L MitoSOX Red (Life Technologies). Myocytes were permeabilized as previously described [25], using saponin (0.01%) added to a solution containing (in mmol/L): 120 K^+ L-aspartate, 20 KCl, 3 MgATP, 10 phosphocreatine, 1 KH_2PO_4, 5 NaCl, 0.1 EGTA, 0.7 $MgCl_2$, 0.019 $CaCl_2$, 20 HEPES (pH 7.2), 5 units/mL creatine phosphokinase, and 5 μmol/L

Fluo-3 K^+ salt (Life Technologies). The free Ca^{2+} concentration in a solution was calculated using MAXChelator software (Stanford University).

Fluo-3, Fluo-4, DCFDA, and MitoSOX Red were excited at 488 nm, and fluorescence signals were acquired at wavelengths >505 nm in the line scan mode or XY mode of the confocal system. Asante NaTRIUM Green and Asante NaTRIUM Green 2 were excited at 543 nm, and fluorescence was acquired at wavelengths >560 nm in the XY scan mode. Fluorescent images were analyzed using ImageJ software (NIH) and Origin 8.1 (OriginLab).

We used exogenous CaMKII (New England Biolabs) to potentiate Ca^{2+} signals in membrane-permeabilized cardiomyocytes [26]. CaMKII was pre-activated by incubation at 30 °C in a CaMKII reaction buffer supplemented with 100 μmol/L ATP, 1.2 μmol/L calmodulin, and 2 mmol/L $CaCl_2$ for 10 min.

In the experiments on intact cells, myocytes were paced at 1 Hz. Fluorescent signals were recorded after 2 min of pacing before or after drug application. For experiments using membrane-permeabilized cells, fluorescence images were recorded within 5 min after membrane permeabilization. All measurements were done at a temperature of 22–24 °C.

2.5. Western blot analysis

Western blot analyses were performed by a standard method. Antibodies for phospho-CaMKIIδ at threonine 286 and for GAPDH were purchased from Santa Cruz Biotechnology. Antibodies for PLN phosphorylated at threonine 17 and RyR2 phosphorylated at serine 2814 were purchased from Badrilla. To detect oxidized CaMKIIδ, an immune serum with antibodies directed against oxidized M281/M282 (ox-CaMKII) was used (polyclonal rabbit, 1:2500 dilution). Secondary antibody was horseradish peroxidase-linked goat anti-rabbit (1:1000) (PerkinElmer Life and Analytical Sciences). The relative intensity of individual bands from Western blots was quantitated using ImageJ software and normalized to GAPDH. The ratio for control was assigned a value of 1.

2.6. TAC mouse model of HF

Transverse aortic constriction (TAC) was performed on 3-month-old male CD-1 mice as previously described [27]. The presence of a TAC-induced pressure gradient across the aortic constriction was verified using echocardiography. Serial echocardiography was done for data acquisition. Two-dimensional guided *m*-mode and 2D images were used to quantify and estimate LV luminal dimensions, systolic and diastolic functions, and fractional shortening. Only mice with an aortic pressure gradient >30 mm Hg were used for experiments. Sham-operated animals were used as controls.

2.7. Statistics

All values were expressed as mean ± SEM. Statistical comparisons were made using unpaired Student's t-test or 2-way ANOVA for repeated measurements ($p < 0.05$).

3. Results

3.1. ATX-II increases I_{NaL} in adult rabbit ventricular myocytes

To increase I_{NaL} in rabbit ventricular myocytes, we superfused cells with 5 nM ATX-II for 30 min. Treatment with ATX-II caused a slowing of the rate of decay of Na^+ current induced by a depolarizing voltage-clamp pulse, thereby increasing I_{NaL} (Fig. 1A). The time constants of I_{Na} decay were 84.6 ± 9.5 ms in ATX-II treated cells and 47.8 ± 9.1 ms in control (vehicle-treated) cells. These results are consistent with previous findings that ATX-II causes slowing and incomplete inactivation of Na^+ channels, and increased I_{NaL} [12,19,28].

3.2. ATX-II increases Na^+ and ROS production, and causes Ca^{2+} mishandling in rabbit ventricular myocytes

The I_{NaL} enhancer ATX-II markedly increased the intracellular Na^+ concentration measured with the fluorescent dye Asante NaTRIUM Green in cardiomyocytes paced at a rate of 1 Hz. The value of F/F_0, the intensity of dye fluorescence in the presence of ATX-II normalized to that before pacing and drug application, was 1.38 ± 0.04 (Fig. 1Bi and Ci). Treatment with the late Na^+ current blockers ranolazine (10 μmol/L), tetrodotoxin (1 μmol/L), and GS-967 (1 μmol/L) in the presence of ATX-II reduced the values of F/F_0 to 1.16 ± 0.06, 1.18 ± 0.09, and 1.1 ± 0.04, respectively (Fig. 1Ci).

ATX-II also significantly increased the cytosolic ROS level (Fig. 1Bii and Cii). The F/F_0 value of DCFDA fluorescence was significantly increased from 1.02 ± 0.04 in control to 1.15 ± 0.02 in the presence of ATX-II (Fig. 1Cii). Application of ranolazine, TTX or GS-967 significantly reduced cellular ROS production in the presence of ATX-II (F/F_0 values were 1.05 ± 0.03, 1.06 ± 0.06 and 1.05 ± 0.05, respectively).

Line-scan confocal images of cardiomyocytes loaded with Fluo-4 AM and paced at 1 Hz revealed an increase in the diastolic Ca^{2+} level in the presence of ATX-II. The value of F/F_0 was increased from 1.0 ± 0.01 in control to 1.78 ± 0.09 in the presence of ATX-II (Fig. 1Biii and Ciii). Inhibition of Na^+ influx with ranolazine, TTX or GS-967 significantly decreased the diastolic Ca^{2+} level in the presence of ATX-II; the values of F/F_0 were 1.16 ± 0.06 (RAN), 1.19 ± 0.09 (TTX) and 1.09 ± 0.07 (GS-967), respectively (Fig. 1Ciii). ATX-induced spontaneous arrhythmic Ca^{2+} releases was also blocked by ranolazine (see Ca^{2+} transients in Fig. 1Biii).

3.3. Both ROS production and CaMKIIδ activation are essential for ATX-II-induced abnormal intracellular Ca^{2+} handling

To determine whether intracellular Ca^{2+} mishandling depends on Na^+-induced oxidative stress, we applied antioxidants to ATX-II-treated rabbit cardiomyocytes (Fig. 2A, B). ATX-II alone increased the number of Ca^{2+} transients and the diastolic Ca^{2+} level (Fig. 2A, B). ATX-II also increased the rate of leak of Ca^{2+} from the SR (Supplemental Fig. 1). Either dithiothreitol (DTT, 5 mmol/L) or coenzyme Q10 (CoQ10, 10 μmol/L) significantly attenuated an ATX-II-induced increase in diastolic Ca^{2+} concentration, restored Ca^{2+} transient amplitude, and eliminated cellular arrhythmias (Fig. 2A, B). CoQ10 also reduced cytosolic Na^+ levels in ATX-II-treated cardiomyocytes (Supplemental Fig. 2).

Next we determined whether CaMKIIδ is involved in ATX-II-induced Ca^{2+} mishandling. Application of a CaMKII inhibitor, either autocamtide inhibitory peptide (AIP, 1 μmol/L) or KN-93 (3 μmol/L), improved intracellular Ca^{2+} handling in ATX-II-treated cells (Fig. 2A, B). By contrast, KN-92, a non-active analog of KN-93, had no effect. Western blot analysis revealed an increase in oxidation of CaMKIIδ at Met281/282 and autophosphorylation of CaMKIIδ at Thr287 (Fig. 2C, D) in the presence of 5 nmol/L ATX-II (Fig. 2C). Antioxidants DTT and CoQ10 prevented the oxidation and phosphorylation of CaMKII in ATX-II-treated cells (Fig. 2C, D). The effect of KN-93 (but not KN-92) was similar to that of the antioxidants. Furthermore, DTT, CoQ10 and KN-93 reduced phosphorylations of CaMKIIδ targets, RyR2 at serine 2814 and PLN at serine 17 (Fig. 2C, D), in the presence of ATX-II. These results suggest that ATX-II-induced ROS production may activate CaMKII.

3.4. Elevated Na^+ modulates Ca^{2+} handling in membrane-permeabilized cardiomyocytes

To rule out the possibility that ion channels, Ca^{2+} pumps and NCX in the sarcolemmal membrane may explain the effects of ATX-II and increased cytosolic $[Na^+]_i$ on intracellular Ca^{2+} handling in this study, we used membrane-permeabilized cardiomyocytes that allow us to control cytosolic Na^+ and Ca^{2+} concentrations. We clamped the

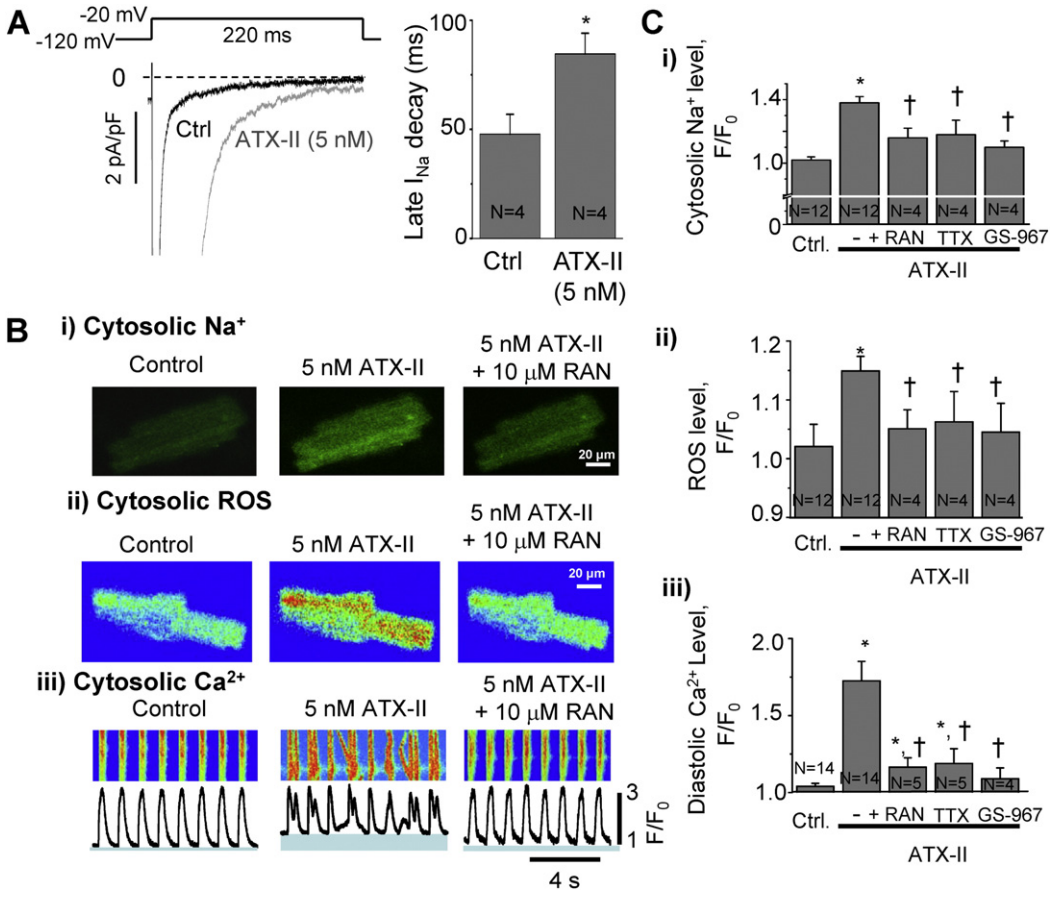

Fig. 1. Activation of I_{NaL} by ATX-II in rabbit ventricular myocytes. i) Representative recordings of I_{NaL} in the absence of drug (control) and after superfusion with 5 nM ATX-II. ii) Mean values of I_{NaL} decay time constant in control and after superfusion with 5 nM ATX-II (N = 4). B. Confocal images of a rabbit ventricular myocyte paced at 1 Hz and loaded with Na^+ dye Asante NaTRIUM Green AM. (i). Application of ATX-II for 2 min increased cytosolic Na^+ compared to control (Ctrl). This effect was reversed by ranolazine (RAN, 10 μmM). ii) Cytosolic ROS, measured using DCFDA, was increased in response to ATX-II, and was also reduced by treatment with RAN. iii) Line-scan recordings of Ca^{2+} transients using the dye Fluo-4 AM. ATX-II increased spontaneous Ca^{2+} release and increased diastolic Ca^{2+} level (shown in blue under each Ca^{2+} transient profile). ATX-II effects on Ca^{2+} transients were reversed by RAN. C. Quantification of results for ATX-II-induced changes in i) cytosolic Na^+, ii) cytosolic ROS, and iii) diastolic Ca^{2+} levels in the absence and presence of RAN (10 μM), TTX (1 μM) and GS-967 (1 μM). Data are normalized to F_0 — the baseline fluorescence signal at the beginning of an experiment. N = 3–14, *p < 0.05 vs control; †p < 0.05 vs ATX-II.

cytosolic free Ca^{2+} concentration at 100 nmol/L with 50 μmol/L EGTA. In the presence of 5 mmol/L Na^+, a rhythmic pattern of spontaneous Ca^{2+} transients is observed in membrane-permeabilized myocytes (Fig. 3A and reference [25]). Elevation of the intracellular Na^+ concentration from a physiological (5 mmol/L) to a pathological (20 mmol/L) level resulted in an accelerated rate of spontaneous Ca^{2+} waves (Fig. 3A). The presence of CoQ10 prevented such an acceleration (Fig. 3B). The finding suggests that ROS plays a role in activation of Ca^{2+} release from intracellular stores (e.g., sarcoplasmic reticulum) when the intracellular Na^+ concentration is raised. Activation of CaMKII by ROS is a potential mechanism of the effect. To verify the involvement of CaMKII in the response to 20 mmol/L Na^+, we pre-treated cells with the CaMKII inhibitor KN-93 (3 μmol/L). KN-93 (but not KN-92) abolished acceleration of spontaneous Ca^{2+} waves induced by 20 mmol/L Na^+ (Fig. 3C). As positive controls, permeabilized myocytes were incubated with exogenous pre-activated CaMKII (2 units activity/mL) or H_2O_2 (100 μmol/L); these agents also induced an acceleration of the frequency of spontaneous Ca^{2+} releases (Supplemental Figs. 3 and 4).

An increase in intracellular Na^+ can cause Ca^{2+} efflux from mitochondria, and has the potential to increase mitochondrial ROS production. Therefore, we used the mitochondria-specific ROS indicator MitoSOX Red to assess ROS production in mitochondria in membrane-permeabilized cardiomyocytes exposed to 5 and 20 mmol/L Na^+. The fluorescence of MitoSOX Red was increased to 173 ± 15% of initial fluorescence intensity in response to elevation of Na^+ from 5 to 20 mmol/L (Supplemental Fig. 5). Inhibition of mitochondrial Na^+–Ca^{2+} exchange with 10 μmol/L CGP-37157 abolished the effect of 20 mmol/L Na^+ on the frequency of intracellular Ca^{2+} transients (Fig. 3C). These data are in accordance with previous observations [6,10].

3.5. Na^+ overload and oxidative stress in mouse TAC model of HF

To confirm whether Na^+ overload can cause ROS production and increase in diastolic Ca^{2+} in the failing heart, we isolated cardiomyocytes from TAC mice with failing hearts. At 4 weeks after TAC, the mice developed cardiac hypertrophy (a 38% increase in the ratio of heart/body weight) and fractional shortening of LV myocardium was reduced (Fig. 4A). It has been shown previously that the level of phosphorylation of CaMKII is increased in TAC hearts [29]. To determine whether TAC intervention changed oxidation of CaMKII we carried out Western blot analysis, which showed a significant increase in ox-CaMKII in TAC cardiac tissue when compared to sham tissue (Fig. 4B). The level of intracellular Na^+ in paced myocytes isolated from TAC animals was significantly reduced by ranolazine (10 μmol/L) or TTX (1 μmol/L) (Fig. 4C) as indicated by decreases in fluorescence of the Na^+-sensitive dye Asante NaTRIUM Green-2 to 74% and 78% of baseline, respectively. Neither ranolazine nor TTX reduced dye fluorescence in myocytes isolated from sham-operated animals (Supplemental Fig. 6). The antioxidant CoQ10 (10 μmol/L) and the CaMKII inhibitor KN-93 (3 μmol/L), but not KN-92, also significantly decreased Asante NaTRIUM

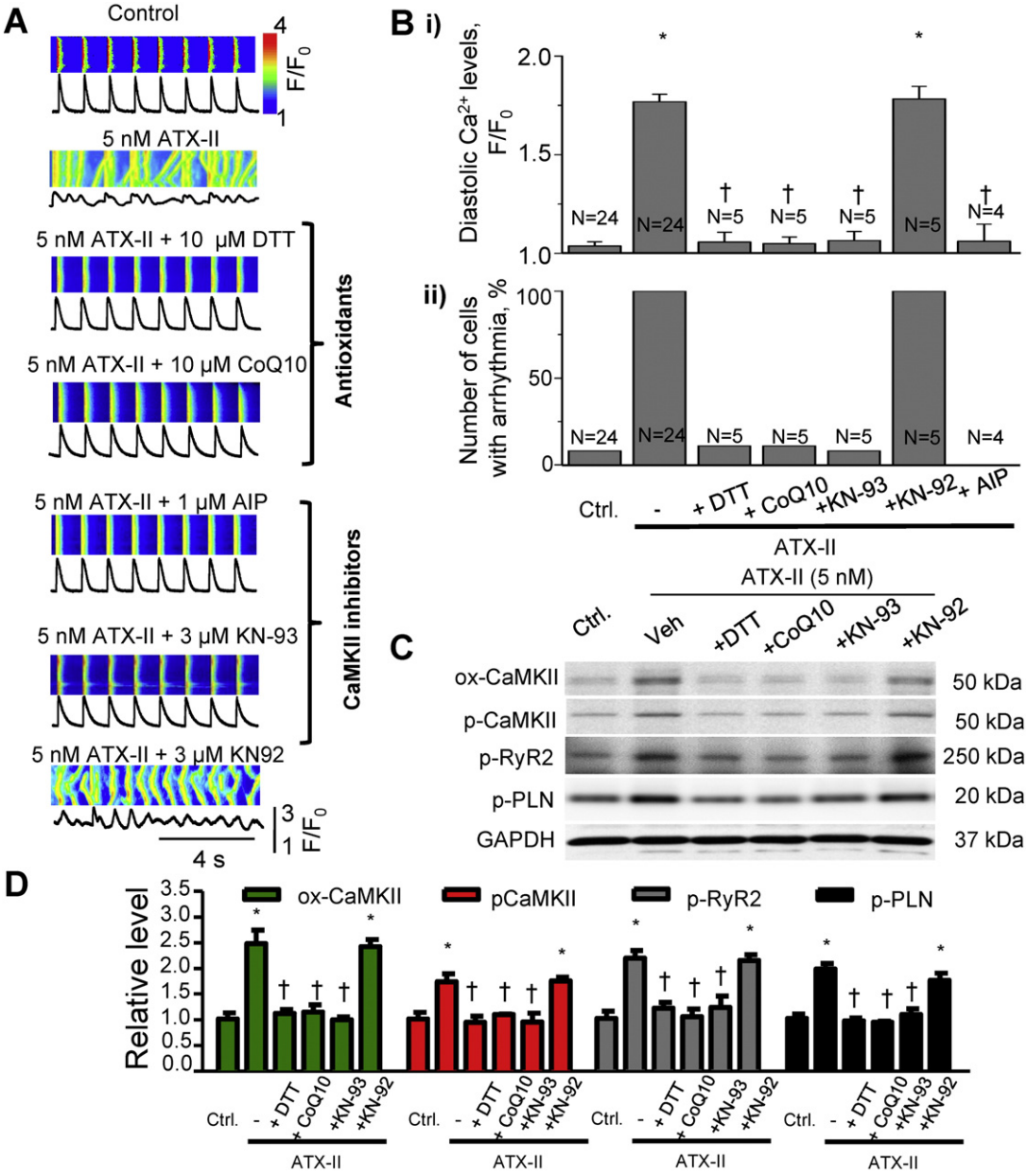

Fig. 2. ATX-II-induced Ca^{2+} mishandling is reversed by antioxidants or CaMKII inhibition. A. Line-scan confocal images of Ca^{2+} transients recorded from paced adult rabbit cardiomyocytes. The antioxidants CoQ10 (10 μM) and DTT (5 mM) or the CaMKII inhibitors, AIP (1 μmM) or KN-93 (3 μM), were applied after induction of arrhythmic Ca^{2+} transients with 5 nM ATX-II. Treatment with antioxidants or CaMKII inhibitors restored normal Ca^{2+} dynamics and attenuated arrhythmic Ca^{2+} transients. KN-92 (3 μM) was used as a negative control for KN-93. B. Quantification of i) diastolic Ca^{2+}, and ii) number of cells with arrhythmic Ca^{2+} transients (%). N = 4–24; *p < 0.05 vs control; †p < 0.05 vs ATX-II alone. C. Western blots for oxidation of CaMKII at Met281/282 (ox-CaMKII), phosphorylation of CaMKII at Thr287 (p-CaMKII), phosphorylation of RyR2s at Ser2814 (p-RyR2) and phosphorylation of PLN at Thr17 (p-PLN). Cardiomyocytes were treated with 5 nM ATX-II, in the absence and presence of antioxidants CoQ10 (10 μM), DTT (5 mM), the CaMKII inhibitor KN-93 (3 μM) and the inactive analog, KN-92 (3 μM). D. Western blot quantification, normalized to GAPDH (N = 3, *p < 0.05 vs control and †p < 0.05 vs ATX-II alone).

Green-2 fluorescence relative to baseline in paced myocytes isolated from TAC mice (Fig. 4C). Treatment of TAC myocytes with ranolazine (10 μmol/L) or TTX (1 μmol/L) also significantly decreased the fluorescence of DCFDA (a ROS-sensitive fluorescent indicator) by 72% and 80% relative to baseline, respectively (Fig. 4D). The fluorescence of DCFDA was also decreased to 69% of baseline by CoQ10 (10 μmol/L) (Fig. 4D). However, inhibition of CaMKII with KN-93 (3 μmol/L) did not significantly change the ROS level (Fig. 4D). None of the studied drugs had an effect on basal Na^+ and ROS levels in myocytes isolated from sham-operated animals (Supplemental Fig. 6).

Analysis of Ca^{2+} transients in myocytes isolated from sham-operated and TAC animals indicated that the rise time of the transient was significantly longer in the TAC group (Supplemental Table 1). Spontaneous Ca^{2+} releases following the termination of 1-Hz stimulations occurred more often in myocytes from TAC than in those isolated from sham animals (Fig. 4E). Inhibition of I_{NaL} by ranolazine (1 μmol/L) or CaMKII with KN-93 (3 μmol/L) normalized Ca^{2+} transients and diminished spontaneous Ca^{2+} waves in TAC myocytes (Fig. 4E, Supplemental Table I) whereas KN-92 (3 μmol/L) had no effect.

4. Discussion

The goal of the present study was to elucidate potential pathways that connect the increases of I_{NaL} and of the cytosolic Na^+ concentration (i.e., Na^+ overload) to disruption of intracellular Ca^{2+} storage and release (dysfunctional Ca^{2+} handling). The major findings were: 1) increases of I_{NaL} and $[Na^+]_i$ promoted ROS generation, CaMKII oxidation and phosphorylation, and phosphorylation of CaMKII substrates,

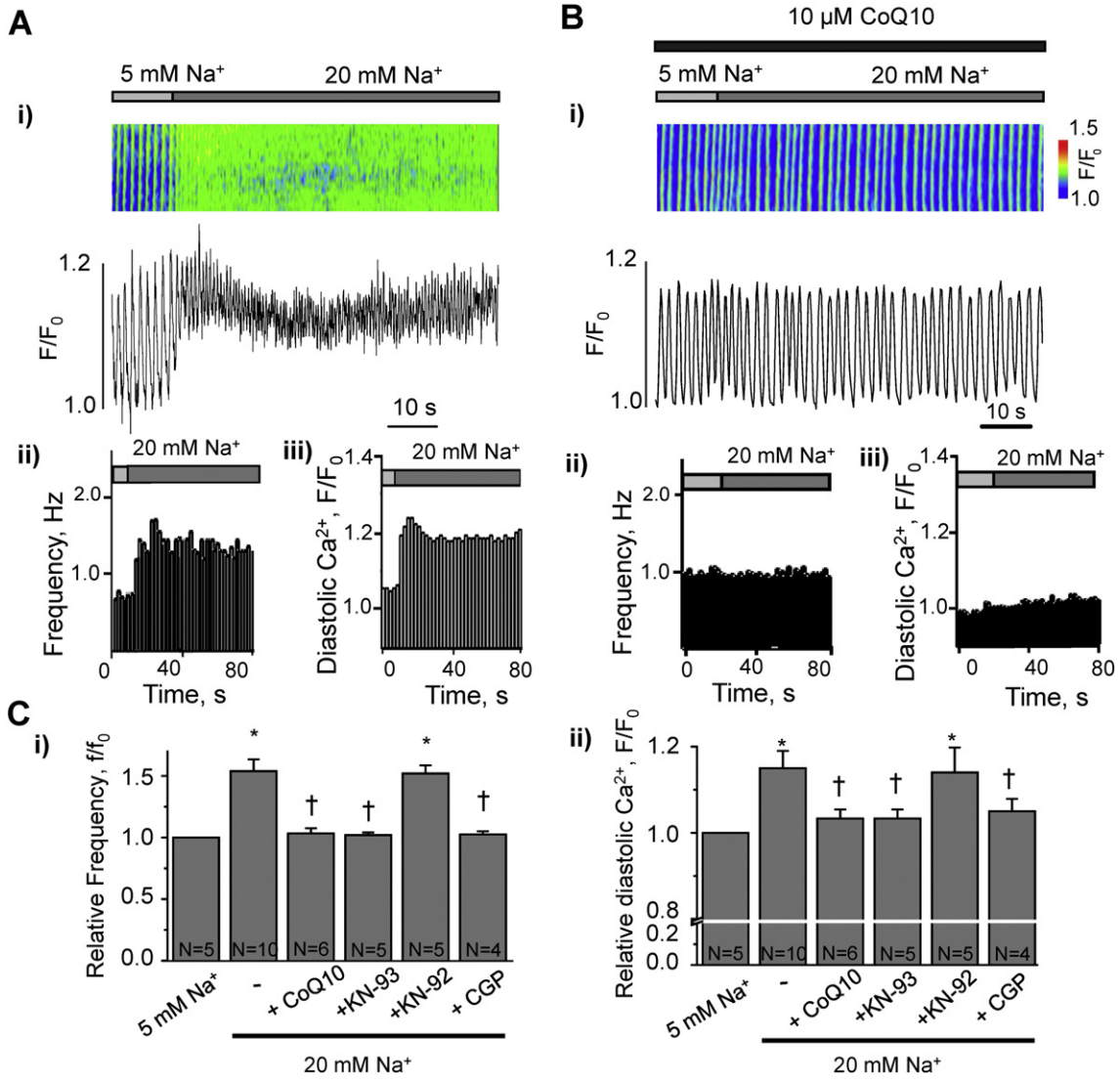

Fig. 3. Role of ROS, mitochondrial Na^+–Ca^{2+} exchange, and CaMKII in maladaptive Ca^{2+} handling induced by elevation of $[Na^+]_i$ in membrane-permeabilized cardiomyocytes: A. i) Confocal line-scan image and profile of Ca^{2+} transients in a membrane-permeabilized rabbit ventricular myocyte, recorded during elevation of cytosolic Na^+ from 5 to 20 mM; ii) spontaneous Ca^{2+} wave frequency and iii) diastolic Ca^{2+} level for the experiment shown in panel (i). B. i. Confocal line-scan image and profile of Ca^{2+} transients in a membrane-permeabilized rabbit ventricular myocyte during elevation of cytosolic Na^+ from 5 to 20 mM in the presence of the antioxidant CoQ10 (10 μmM); ii) spontaneous Ca^{2+} wave frequency and iii) diastolic Ca^{2+} level for the experiment shown in (i). C. Quantification of spontaneous Ca^{2+} wave frequency f/f_0 (i) and the diastolic Ca^{2+} level (ii), induced by elevation of $[Na^+]_i$ in the absence and presence of the antioxidant CoQ10 (10 μM), the CaMKII inhibitor KN-93 (3 μM), the inactive analog KN-92 (3 μM) or mitochondrial Na^+–Ca^{2+} exchange inhibitor CGP-37157 (CGP, 10 μM) N = 4–10, *$p < 0.05$ vs control; †$p < 0.05$ vs 20 mM Na^+. f_0, the frequency of spontaneous Ca^{2+} waves at the beginning of the experiment.

including RyR2; 2) an increase of $[Na^+]_i$ caused increases of diastolic Ca^{2+} and the frequency of spontaneous Ca^{2+} waves in membrane-permeabilized myocytes, i.e., in the absence of sarcolemmal membrane regulation of the intracellular Ca^{2+} concentration; 3) Ca^{2+} mishandling induced by Na^+ overload was reversed by ranolazine and tetrodotoxin, CaMKII inhibitors, antioxidants, and inhibition of the mitochondrial Na^+–Ca^{2+} exchanger; 4) in cardiomyocytes isolated from failing hearts of TAC mice, intracellular levels of Na^+ and ROS were reduced by inhibitors of I_{NaL} and by CoQ10, and inhibition of CaMKII reduced the frequency of spontaneous Ca^{2+} release events. Taken together, the results suggest a pathological pathway (Fig. 5) whereby cardiomyocyte Na^+ overload promotes mitochondrial ROS generation, resulting in CaMKII oxidation and phosphorylation, and CaMKII-mediated phosphorylation of substrates including RyR2, which increases Ca^{2+} leak from SR (Supplemental Fig. 1) and the frequency of SR Ca^{2+} release events (Figs. 1, 2), resulting in an increase of the cytosolic Ca^{2+} concentration during diastole (Figs. 1, 2, 5). This pathway appears to be operative in myocytes of failing hearts. Our findings are consistent with and expand on the previously reported links between cytosolic Na^+ overload and mitochondrial ROS generation [6,7] and between oxidized CaMKII and Ca^{2+} overload [2,11,12,18,30,31].

4.1. Contribution of I_{NaL} to Na^+ influx

In the present research we used I_{NaL} enhancement (Fig. 1) as a tool to increase cytosolic Na^+ load. I_{NaL} that occurs during the plateau of the action potential has been shown by many investigators to cause AP prolongation. I_{NaL} can account for 30% or more of Na^+ influx through myocyte Na^+ channels [32]. Other potential sources of Na^+ entry via Na^+ channels are "window current" [33], and "background current" near the threshold of Na^+ channel activation [34]. They are not usually called I_{NaL}, which typically refers to current at plateau potentials due to failure of open state inactivation of Na^+ channels, but they can be blocked by ranolazine and TTX and may have contributed to Na^+ entry in this study. The effects of CaMKII, oxidation, and diseases on window and background Na^+ currents are poorly understood.

Our results indicate that the decay time constant of I_{NaL} in ATX-II (5 nM)-treated rabbit cardiomyocytes was prolonged 1.5–2-fold. This

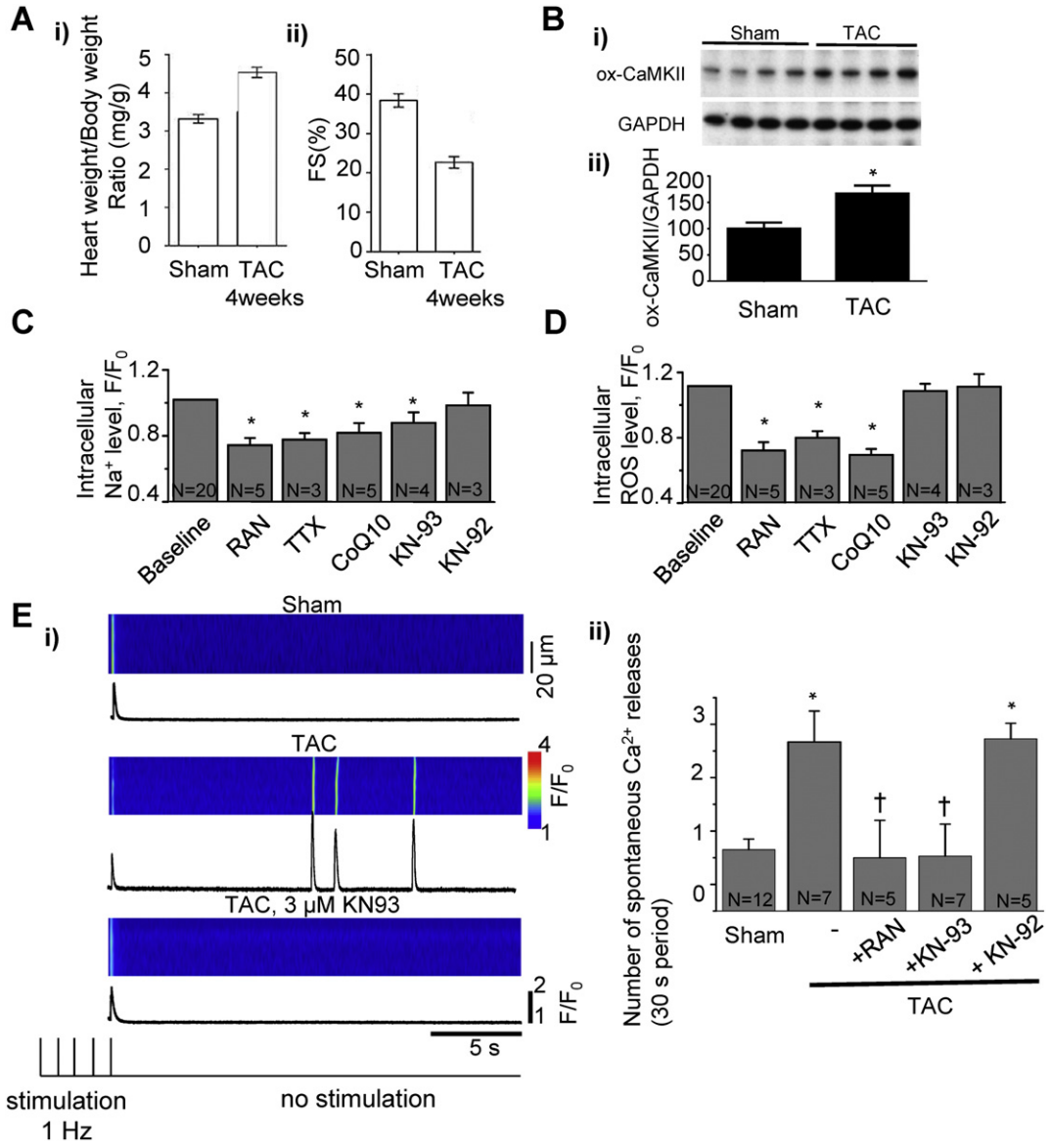

Fig. 4. Pathological contributions of I_{NaL}, CaMKII and ROS to maladaptive Ca^{2+} handling in cardiomyocytes isolated from mouse failing hearts. A. i) Heart weight/body weight ratio and ii) fractional shortening (FS, %) of the left ventricular wall in male CD-1 mice subjected to transverse aortic constriction (TAC) for 4 weeks, compared to sham-operated, age-matched controls (sham). B. i) Western blots for oxidation of CaMKII at Met281/282 (ox-CaMKII) and Western blot quantification, normalized to GAPDH (ii). Effects of ranolazine (10 μM), TTX (1 μM), CoQ10 (10 μM), KN-93 (3 μM), and KN-92 (3 μM) on levels of intracellular Na^+ (C) and ROS (D) in myocytes isolated from TAC mice and paced at a rate of 1 Hz ($N = 3–20$, $p < 0.05$), compared to baseline. E. Spontaneous Ca^{2+} release events following termination of 1 Hz stimulation of myocytes isolated from sham-operated and TAC mice in the absence or presence of RAN (10 μM), KN-93 (3 μM) or its inactive analog KN-92 (3 μM). *$p < 0.05$ vs sham and †$p < 0.05$ vs TAC without drugs.

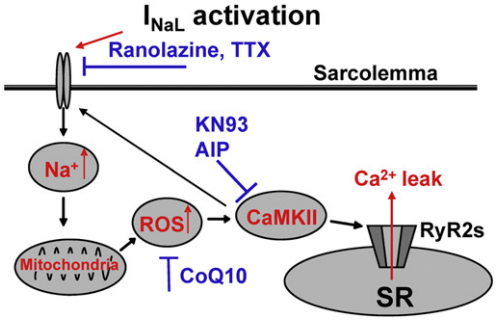

Fig. 5. Proposed mechanism for I_{NaL}-mediated Na^+ overload-induced disruption of myocyte Ca^{2+} handling. An increase of I_{NaL} leads to an increase of $[Na^+]_i$. Cytosolic Na^+ overload attenuates mitochondrial Ca^{2+} uptake via the mitochondrial Na^+/Ca^{2+} exchanger, thereby reducing NADPH regeneration and increasing mitochondrial ROS. ROS oxidizes and activates CaMKII, resulting in phosphorylation of the CaMKII substrate RyR2 and increasing Ca^{2+} leak from sarcoplasmic reticulum (SR).

prolongation is similar in magnitude to that found in myocytes from failing hearts in TAC mice [29]. This suggests that the increase of I_{NaL} is comparable in both models. Therefore, we believe that the effect of ATX-II on rabbit myocytes in this study is not so large as to be irrelevant to an understanding of its potential pathological effects in failing hearts, and to the mechanisms by which the effect of Na^+ overload (regardless of its cause) is mediated.

4.2. Na^+ overload induced mitochondrial ROS generation

The detrimental influence of intracellular Na^+ overload on cardiac cell function is well recognized [3–5,8,12,19–21]. The prevailing view of the pathway that connects cytosolic Na^+ accumulation to altered Ca^{2+} homeostasis has focused on the role of the sarcolemmal Na^+–Ca^{2+} exchanger in regulation of the cytosolic Ca^{2+} concentration. In this pathway, Na^+ overload decreases Ca^{2+} extrusion and increases Ca^{2+} entry via the exchanger, causing Ca^{2+} accumulation that results

in contractile dysfunction and arrhythmias. The results of the present study do not dispute the validity of this mechanism. However, our results suggest that mechanisms independent of membrane Na^+–Ca^{2+} exchange also appear to take part in Na^+ overload-induced dysregulation of Ca^{2+} homeostasis. The finding that ATX-II, an enhancer of I_{NaL}, increased cytosolic Na^+, diastolic Ca^{2+}, ROS, the frequency of spontaneous Ca^{2+} release events, and oxidation and phosphorylation of CaMKII strongly suggest that I_{NaL} can raise the level of cytosolic Na^+ sufficiently to disrupt Ca^{2+} homeostasis. Importantly, we demonstrate that in the absence of a functional plasma membrane (i.e., in membrane-permeabilized adult rabbit cardiomyocytes) elevation of cytosolic Na^+ alone is sufficient to provoke increases in ROS generation, the frequency of Ca^{2+} waves, and the diastolic Ca^{2+} concentration (Fig. 3).

Our observations that ATX-II promotes elevated ROS production (Fig. 1) and that deleterious consequences of Na^+ overload are attenuated by antioxidants such as CoQ10 and DTT (Figs. 2, 3) are in agreement with a growing body of evidence demonstrating that Na^+ overload promotes cellular oxidative stress. Kohlhaas et al. [7] recently described a series of experiments demonstrating that elevation of cytosolic Na^+ is sufficient to induce mitochondrial ROS generation. In patch clamped guinea-pig cardiomyocytes, elevation of cytosolic Na^+ from 5 to 15 mmol/L resulted in mitochondrial Ca^{2+} extrusion with a concurrent increase in H_2O_2 generation, effects which were blocked by the mitochondrial Na^+–Ca^{2+} exchange inhibitor CGP-37157 [7]. These authors [7] suggest that Na^+ overload promotes mitochondrial Ca^{2+} efflux, resulting in H_2O_2 accumulation as a consequence of impaired NADPH-dependent mitochondrial antioxidant capacity. In our study, using permeabilized myocytes, we confirmed that Na^+ overload can increase mitochondrial ROS production (Supplemental Fig. 5) and that Na^+-induced Ca^{2+} mishandling is attenuated by CGP-37157 (Fig. 3C), in agreement with Kohlhaas et al. [7]. Involvement of the mitochondrial Na^+–Ca^{2+}exchanger in this mechanism assumes that mitochondrial Na^+ and Ca^{2+} concentrations should be altered by cytosolic Na^+ overload. Changes in either Na^+ or Ca^{2+} concentration can induce mitochondrial dysfunction. Reduction of mitochondrial Ca^{2+} efflux in Na^+-overloaded myocytes may explain effect of ranolazine (which can reduce I_{NaL} and the cytosolic Na^+ concentration [19,20] and can indirectly increase the activity of mitochondrial dehydrogenases such as pyruvate dehydrogenase that rely on mitochondrial Ca^{2+} for their activity [35,36]). However, it should be noted that the mechanisms of increased mitochondrial ROS generation are only partially understood.

4.3. Elevation of $[Na^+]_i$, CaMKII oxidation and phosphorylation, and their relationship to disruption of Ca^{2+} handling

A novel observation in this study was that CaMKII oxidation was increased subsequent to an elevation by ATX-II of the intracellular Na^+ concentration in intact cardiomyocytes (Fig. 2C, D) and TAC cardiac tissue (Fig. 4B). ATX-II-induced CaMKII oxidation was detected using an antibody that specifically recognizes the oxidized methionine 281/282 site on CaMKII [30]. In parallel to the increase in oxidized-CaMKII, we observed an ATX-II-induced increase in CaMKII phosphorylation at Thr287, demonstrating increased autophosphorylation (Fig. 2C, D). These results are in agreement with previous studies demonstrating that CaMKII oxidation is accompanied by an increase in CaMKII autophosphorylation [11,30,31]. Importantly, the increases in CaMKII oxidation and phosphorylation were accompanied by an elevation in the phosphorylation of CaMKII substrates involved in Ca^{2+} handling, including PLN and RyR2 (Fig. 2C, D), demonstrating functional activation of CaMKII. The ATX-II-induced oxidation/phosphorylation of CaMKII and its substrates was attenuated by inhibitors of I_{NaL}, antioxidants (DTT or CoQ10), or the CaMKII inhibitor KN-93. Treatment of myocytes with KN-93 or CoQ10 restored normal Ca^{2+} dynamics and attenuated arrhythmic activity in the presence of ATX-II (Fig. 2B). Similarly, KN-93 and CoQ10 also prevented aberrant Ca^{2+} handling induced by elevated cytosolic Na^+ in permeabilized cardiomyocytes (Fig. 3). Furthermore, treatment of permeabilized cells with exogenous, pre-activated phosphorylated CaMKII accelerated the frequency of spontaneous Ca^{2+} waves and increased diastolic Ca^{2+} (Supplemental Fig. 3). The effects of pre-activated CaMKII were strikingly similar to those observed after elevation of the intracellular Na^+ concentration in permeabilized myocytes (Fig. 3). Taken together, our data provide evidence that CaMKII activity is both necessary and sufficient to induce maladaptive Ca^{2+} handling in cardiomyocytes, and it acts as both a sensor for, and an effector of responses to, an increase in ROS production [11,30,31].

A high level of oxidized CaMKIIδ has been associated with disruption of intracellular Ca^{2+} handling, arrhythmias, and contractile dysfunction [18,30,31,37–39]. Recently, Wagner et al. [18] demonstrated that ROS-activated CaMKII is required for I_{NaL} augmentation leading to cellular Na^+ and Ca^{2+} overload. CaMKII can phosphorylate the cardiac Na^+ channel pore-forming alpha subunit and enhance I_{NaL} [13,18,40]. Thus, intracellular Na^+-dependent activation of CaMKII could induce further activation of I_{NaL} by a positive feedback mechanism. Moreover, CaMKII alters Ca^{2+} handling in cardiac myocytes via phosphorylation of RyR2 and phospholamban to increase Ca^{2+} release from, and Ca^{2+} loading of, the sarcoplasmic reticulum [41]. The finding that oxidation and phosphorylation of CaMKII were increased in myocytes exposed to the I_{NaL} enhancer ATX-II is in accord with previous reports [12]. Thus, CaMKII activation, including activation through an oxidation-dependent pathway, is a key element in a complex interplay between Na^+ load and Ca^{2+} handling under pathological conditions [12,17,18,31,38,39].

4.4. TAC data and relevance to heart failure

Increases of I_{NaL} and CaMKII activity are well documented in cardiomyocytes isolated from failing hearts of experimental animals [5,17,20,42] and human patients [20,42]. Toischer et al. recently reported roles for I_{NaL} and CaMKII in the progression of pressure-overload induced heart disease after TAC in mice [29]. In their study, I_{NaL} was not enhanced during the compensatory hypertrophy stage (1 week post-TAC) but was significantly enhanced in hearts that had developed heart failure (5 weeks post-TAC) characterized by a reduced ejection fraction. In parallel to the increase in I_{NaL} observed in failing myocytes, there was a significant increase in both CaMKII autophosphorylation and phosphorylation of $Na_V1.5$ at the CaMKII site ser-571, when compared to myocytes isolated from non-failing hearts or from hearts in the compensatory hypertrophy stage [29]. In the present study, we utilized a similar model of pressure overload-induced heart failure in mice to examine the contributions of I_{NaL}, CaMKII and ROS to maladaptive Ca^{2+} handling in the failing heart. Heart failure was induced by 4 weeks TAC, as evidenced by a significant reduction in fractional shortening of left ventricular myocardium, relative to sham-operated mice (Fig. 4A). Importantly, the level of ox-CaMKII was increased in cardiac tissue of TAC animals relative to sham animals (Fig. 4B). Cardiomyocytes isolated from failing hearts had evidence of maladaptive Ca^{2+} handling, manifested as an increase in spontaneous Ca^{2+} release events (Fig. 4D). The frequency of Ca^{2+} release events was normalized after treatment of myocytes with I_{NaL} inhibitor ranolazine or CaMKII inhibitor KN-93. Treatment with ranolazine, KN-93 or CoQ10 all reduced cellular Na^+, whereas ROS was reduced by either CoQ10 or ranolazine, but not by KN-93, because elevation of ROS production can occur in the absence of CaMKII activation (Fig. 5). None of these agents had an effect on the cytosolic Na^+ concentration or on ROS production in myocytes isolated from non-failing hearts (Supplemental Fig. 6). Taken together with the work of Toischer et al. [29] our findings suggest that I_{NaL}-induced Na^+ overload, oxidative stress, and CaMKII activity likely contribute to pro-arrhythmic Ca^{2+} mishandling in the failing heart.

5. Conclusions

Our results provide experimental evidence that CaMKIIδ oxidation subsequent to mitochondrial ROS generations induced by cytosolic Na^+ overload is an important component of an intracellular signaling pathway (Fig. 5) leading to aberrant Ca^{2+} handling under pathologic conditions such as heart failure. This pathway is not dependent on, but may operate in parallel with, the "classical" mechanism of Na^+-induced Ca^{2+} overload mediated by the sarcolemmal Na^+–Ca^{2+} exchanger. The evidence that Na^+ overload-induced mitochondrial ROS formation and CaMKII oxidation are mechanisms of potential importance in the etiology of cardiac disease may provide a conceptual framework for the development of new drug therapies.

Abbreviations

AIP	autocamtide inhibitory peptide
ATX-II	*Anemonia sulcata* toxin-II
Ca^{2+}	calcium
CaMKIIδ	calcium/calmodulin dependent protein kinase II delta
CGP	CGP-37157
CoQ10	coenzyme Q10
DTT	dithiothreitol
I_{Na}	sodium channel current
I_{NaL}	sodium channel late current
Na^+	sodium
NCX	sarcolemmal sodium–calcium exchanger
PLN	phospholamban
RAN	ranolazine
ROS	reactive oxygen species
RyR2	ryanodine receptor 2
SR	sarcoplasmic reticulum
TAC	transverse aortic constriction
TTX	tetrodotoxin

Disclosures

Serge Viatchenko-Karpinski, Dmytro Kornyeyev, Nesrine El-Bizri, Grant Budas, Peidong Fan, Zhan Jiang, Luiz Belardinelli and Lina Yao are full time employees of Gilead Sciences Inc. John C. Shryock is a former employee of Gilead Sciences Inc.

Acknowledgments

The authors especially thank Sridharan Rajamani (Gilead Sciences Inc.) for the experimental assistance.

This project was funded by a grants from the National Institutes of Health (NIH) Grants R01-HL079031, R01-HL096652, R01-HL070250 and R01-HL071140 (all — Marc E. Anderson) and by a grant from Gilead Sciences Inc. (C.P. Chang).

Appendix A. Supplementary data

Supplementary data to this article can be found online at http://dx.doi.org/10.1016/j.yjmcc.2014.09.009.

References

[1] Bers DM. Calcium cycling and signaling in cardiac myocytes. Annu Rev Physiol 2008;70:23–49.
[2] Murphy E, Eisner DA. Regulation of intracellular and mitochondrial sodium in health and disease. Circ Res 2009;104:292–303.
[3] Noble D, Noble PJ. Late sodium current in the pathophysiology of cardiovascular disease: consequences of sodium–calcium overload. Heart 2006;92(Suppl. 4):iv1–5.
[4] Belardinelli L, Shryock JC, Fraser H. Inhibition of the late sodium current as a potential cardioprotective principle: effects of the late sodium current inhibitor ranolazine. Heart 2006;92(Suppl. 4):iv6–iv14.
[5] Undrovinas NA, Maltsev VA, Belardinelli L, Sabbah HN, Undrovinas A. Late sodium current contributes to diastolic cell Ca^{2+} accumulation in chronic heart failure. J Physiol Sci 2010;60:245–57.
[6] Maack C, Cortassa S, Aon MA, Ganesan AN, Liu T, O'Rourke B. Elevated cytosolic Na^+ decreases mitochondrial Ca^{2+} uptake during excitation–contraction coupling and impairs energetic adaptation in cardiac myocytes. Circ Res 2006;99:172–82.
[7] Kohlhaas M, Liu T, Knopp A, Zeller T, Ong MF, Böhm M, et al. Elevated cytosolic Na^+ increases mitochondrial formation of reactive oxygen species in failing cardiac myocytes. Circulation 2010;121:1606–13.
[8] O'Rourke B, Maack C. The role of Na dysregulation in cardiac disease and how it impacts electrophysiology. Drug Discov Today Dis Models 2007;4:207–17.
[9] Brandes R, Bers DM. Intracellular Ca^{2+} increases the mitochondrial NADH concentration during elevated work in intact cardiac muscle. Circ Res 1997;80:82–7.
[10] Liu T, O'Rourke B. Enhancing mitochondrial Ca^{2+} uptake in myocytes from failing hearts restores energy supply and demand matching. Circ Res 2008;103:279–88.
[11] Erickson JR, He BJ, Grumbach IM, Anderson ME. CaMKII in the cardiovascular system: sensing redox states. Physiol Rev 2011;91:889–915.
[12] Yao L, Fan P, Jiang Z, Viatchenko-Karpinski S, Wu Y, Kornyeyev D, et al. Nav1.5-dependent persistent Na^+ influx activates CaMKII in rat ventricular myocytes and N1325S mice. Am J Physiol Cell Physiol 2011;301:C577–86.
[13] Bers DM, Grandi E. Calcium/calmodulin-dependent kinase II regulation of cardiac ion channels. J Cardiovasc Pharmacol 2009;54:180–7.
[14] Chelu MG, Sarma S, Sood S, Wang S, Van Oort RJ, Skapura DG, et al. Calmodulin kinase II-mediated sarcoplasmic reticulum Ca^{2+} leak promotes atrial fibrillation in mice. J Clin Invest 2009;119:1940–51.
[15] Couchonnal LF, Anderson ME. The role of calmodulin kinase II in myocardial physiology and disease. Physiology (Bethesda) 2008;23:151–9.
[16] Currie S. Cardiac ryanodine receptor phosphorylation by CaM kinase II: keeping the balance right. Front Biosci 2009;14:5134–56.
[17] Anderson ME, Brown JH, Bers DM. CaMKII in myocardial hypertrophy and heart failure. J Mol Cell Cardiol 2011;51:468–73.
[18] Wagner S, Ruff HM, Weber SL, Bellmann S, Sowa T, Schulte T, et al. Reactive oxygen species-activated Ca/calmodulin kinase IIdelta is required for late I_{Na} augmentation leading to cellular Na and Ca overload. Circ Res 2011;108:555–65.
[19] Song Y, Shryock JC, Wagner S, Maier LS, Belardinelli L. Blocking late sodium current reduces hydrogen peroxide-induced arrhythmogenic activity and contractile dysfunction. J Pharmacol Exp Ther 2006;318:214–22.
[20] Sossalla S, Wagner S, Rasenack EC, Ruff H, Weber SL, Schöndube FA, et al. Ranolazine improves diastolic dysfunction in isolated myocardium from failing human hearts—role of late sodium current and intracellular ion accumulation. J Mol Cell Cardiol 2008;45:32–43.
[21] Shryock JC, Song Y, Rajamani S, Antzelevitch C, Belardinelli L. The arrhythmogenic consequences of increasing late I_{Na} in the cardiomyocyte. Cardiovasc Res 2013;99:600–11.
[22] Chahine M, Plante E, Kallen RG. Sea anemone toxin (ATX II) modulation of heart and skeletal muscle sodium channel alpha-subunits expressed in tsA201 cells. J Membr Biol 1996;152:39–48.
[23] Belardinelli L, Liu G, Smith-Maxwell C, Wang WQ, El-Bizri N, Hirakawa R, et al. A novel, potent, and selective inhibitor of cardiac late sodium current suppresses experimental arrhythmias. J Pharmacol Exp Ther 2013;344:23–32.
[24] Brunner M, Peng X, Liu GX, Ren XQ, Ziv O, Choi BR, et al. Mechanisms of cardiac arrhythmias and sudden death in transgenic rabbits with long QT syndrome. J Clin Invest 2008;118:2246–59.
[25] Lukyanenko V, Viatchenko-Karpinski S, Smirnov A, Wiesner TF, Györke S. Dynamic regulation of sarcoplasmic reticulum $Ca^{(2+)}$ content and release by luminal $Ca^{(2+)}$-sensitive leak in rat ventricular myocytes. Biophys J 2001;81:785–98.
[26] Guo T, Zhang T, Mestril R, Bers DM. Ca^{2+}/calmodulin-dependent protein kinase II phosphorylation of ryanodine receptor does affect calcium sparks in mouse ventricular myocytes. Circ Res 2006;99:398–406.
[27] Hang CT, Yang J, Han P, Cheng HL, Shang C, Ashley E, et al. Chromatin regulation by Brg1 underlies heart muscle development and disease. Nature 2010;466:62–7.
[28] Ulbricht W. Sodium channel inactivation: molecular determinants and modulation. Physiol Rev 2005;85:1271–301.
[29] Toischer K, Hartmann N, Wagner S, Fischer TH, Herting J, Danner BC, et al. Role of late sodium current as a potential arrhythmogenic mechanism in the progression of pressure-induced heart disease. J Mol Cell Cardiol 2013;61:111–22.
[30] Erickson JR, Joiner MA, Guan X, Kutschke W, Yang J, Oddis CV, et al. A dynamic pathway for calcium-independent activation of CaMKII by methionine oxidation. Cell 2008;133:462–74.
[31] Wagner S, Rokita AG, Anderson ME, Maier LS. Redox regulation of sodium and calcium handling. Antioxid Redox Signal 2013;18:1063–77.
[32] Makielski J, Farley AL. Na^+ current in human ventricle: implications for sodium loading and homeostasis. J Cardiovasc Electrophysiol 2006;17:S15–20.
[33] Colatsky TJ. Mechanisms of action of lidocaine and quinidine on action potential duration in rabbit cardiac Purkinje fibers. Circ Res 1982;50:17–27.
[34] Zilberter YI, Starmer F, Starobin J, Grant AO. Late Na channels in cardiac cells: the physiological role of background Na channels. Biophys J 1994;87:153–60.
[35] Clarke B, Spedding M, Patmore L, McCormack JG. Protective effects of ranolazine in guinea-pig hearts during low-flow ischaemia and their association with increases in active pyruvate dehydrogenase. Br J Pharmacol 1993;109:748–50.
[36] Clarke B, Wyatt KM, McCormack JG. Ranolazine increases active pyruvate dehydrogenase in perfused normoxic rat hearts: evidence for an indirect mechanism. J Mol Cell Cardiol 1996;28:341–50.
[37] Purohit A, Rokita AG, Guan X, Chen B, Koval OM, Voigt N, et al. Oxidized CaMKII triggers atrial fibrillation. Circulation 2013;128:1748–57.

[38] Rokita AG, Anderson ME. New therapeutic targets in cardiology: arrhythmias and Ca^{2+}/calmodulin-dependent kinase II (CaMKII). Circulation 2012;126:2125–39.
[39] Swaminathan PD, Purohit A, Hund TJ, Anderson ME. Calmodulin-dependent protein kinase II: linking heart failure and arrhythmias. Circ Res 2012;110:1661–77.
[40] Wagner S, Dybkova N, Rasenack EC, Jacobshagen C, Fabritz L, Kirchhof P, et al. Ca^{2+}/calmodulin-dependent protein kinase II regulates cardiac Na^{+} channels. J Clin Invest 2006;116:3127–38.
[41] Maier LS, Zhang T, Chen L, DeSantiago J, Brown JH, Bers DM. Transgenic CaMKIIdeltaC overexpression uniquely alters cardiac myocyte Ca^{2+} handling: reduced SR Ca^{2+} load and activated SR Ca^{2+} release. Circ Res 2003;92:904–11.
[42] Valdivia CR, Chu WW, Pu J, Foell JD, Haworth RA, Wolff MR, et al. Increased late sodium current in myocytes from a canine heart failure model and from failing human heart. J Mol Cell Cardiol 2005;38:475–83.

Glossary

F/F_0: the intensity of dye fluorescence in the presence of an experimental intervention (e.g., drug application) normalized to the intensity of dye fluorescence in the same preparation before the intervention (i.e., control).